

Limitations in quantum computing from resource constraints

Marco Fellous-Asiani,¹ Jing Hao Chai,² Robert S. Whitney,³ Alexia Auffèves,¹ and Hui Khoon Ng^{4, 2, 5, *}

¹*Institut Néel, Grenoble, France*

²*Centre for Quantum Technologies, National University of Singapore, Singapore*

³*Laboratoire de Physique et Modélisation des Milieux Condensés,
Université Grenoble Alpes and CNRS, BP 166, 38042 Grenoble, France.*

⁴*Yale-NUS College, Singapore*

⁵*MajuLab, International Joint Research Unit UMI 3654,
CNRS, Université Côte d'Azur, Sorbonne Université,*

National University of Singapore, Nanyang Technological University, Singapore

(Dated: December 24, 2020)

Fault-tolerant quantum computation is the only known route to large-scale, accurate quantum computers. Fault tolerance schemes prescribe how, by investing more physical resources and scaling up the size of the computer, we can keep the computational errors in check and carry out more and more accurate calculations. Underlying all such schemes is the assumption that the error per physical gate is independent of the size of the quantum computer. This, unfortunately, is not reflective of current quantum computing experiments. Here, we examine the general consequences on fault-tolerant quantum computation when constraints on physical resources, such as limited energy input, result in physical error rates that grow as the computer grows. In this case, fault tolerance schemes can no longer reduce computational error to an arbitrarily small number, even if one starts below the so-called fault tolerance noise threshold. Instead, there is a minimum attainable computational error, beyond which further growth of the computer in an attempt to reduce the error becomes counter-productive. We discuss simple, but rather generic, situations in which this effect can arise, and highlight the areas of future developments needed for experiments to overcome this limitation.

With the advent of small-scale quantum computing devices from companies like IBM, and the myriad software and hardware quantum startups, the interest in realising quantum computers is at an all-time high. The latest declaration of quantum supremacy by Google [1] begs the question: How do we make our quantum computers more powerful? The answer is, of course, to have larger quantum computers. But larger also usually means noisier, with more fragile quantum components that can go wrong, leading to more computational errors. The way out of this conundrum is fault-tolerant quantum computation (FTQC), the only known route to scaling up quantum computers while keeping errors in check.

FTQC schemes have been known since the early days of the field [2–6], and remain an active field of research, especially with the recent discussions of experimentally feasible surface codes (see, for example, Ref. [7] for a review). Underlying all FTQC schemes are basic assumptions about the nature of the quantum devices and the noise afflicting them. Many of these assumptions, laid down long before experimental devices came about, were based on general physical expectations not specific to any one implementation. As we learn more about the shape of quantum computers to come, it is important to re-visit those assumptions, to update them to properly describe real devices.

FTQC tells us how to scale up the quantum computer, to accommodate larger problem sizes and improve computational accuracy, by increasing the physical resources spent on implementing the computation. Every known

FTQC scheme relies on quantum error correction (QEC) codes to remove errors, using more and more powerful codes to remove more and more errors, accompanied by a prescription to avoid uncontrolled spread of errors as the computer grows. One key assumption is that the physical error probability η —the maximum probability that an error occurs in a physical qubit or gate—remains constant as the computer scales up. If η grows as the computer grows, we cannot expect to keep up with the rapid accumulation of errors.

Unfortunately, the growth of η with scale is observed in current quantum devices. For example, in ion-trap experiments, the gate fidelity drops rapidly if more and more ions are put into the same trap; this is the motivation behind the push for networked ion traps and flying qubits to communicate between traps (see, for example, [8]). Another example is provided by qubits that are coherently controlled, by resonantly addressing their transition. Here a limit on the total available driving power results in lower gate fidelity, if many gates have to be done simultaneously [9].

In this work, we examine the consequences on FTQC of growing physical error probability η as the computer scales up. Fig. 1 presents a cartoon of the typical situation where practical constraints on physical resources lead to increasing η as the computer grows. It should come as no surprise that the standard quantum accuracy threshold theorem [2–6, 10, 11]—a cornerstone result that says that arbitrarily accurate quantum computation is attainable by scaling up the physical computer once the

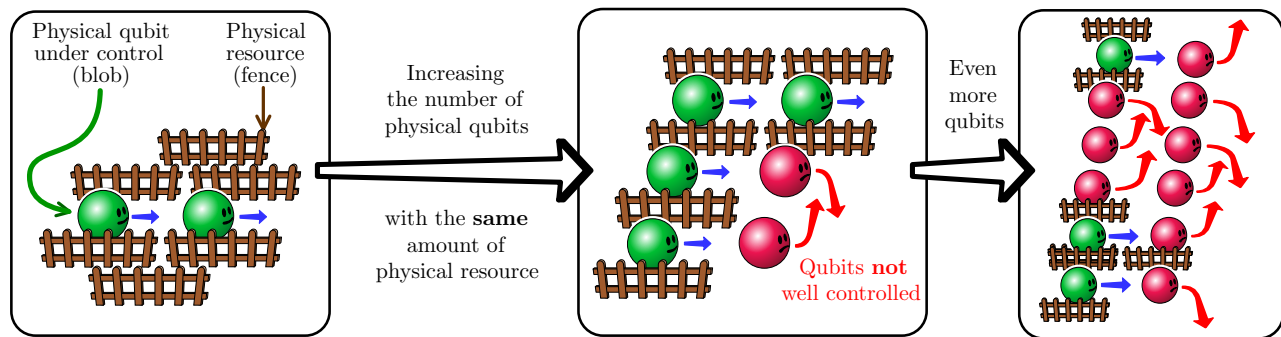


FIG. 1. A cartoon depicting how resource constraints can lead to increased computational errors. Each gate operation on a physical qubit (blob) requires a certain amount of physical resource (fence) for good control. If the number of physical qubits increases as the computer grows, without a proportionate increase in control resource, errors will increase.

noise is below a threshold level—no longer holds. What is startling is how early its failure can set in, and how easily such conditions can arise in real experiments. In one of our examples below (see subsection “Total resource constraints”), for error correction to even be useful, we require a condition on the physical error probability that is 10^5 smaller than the usual fault-tolerance threshold condition. This highlights the areas of current weakness that demand further study, if we want to continue on the road to genuinely useful quantum computers.

ACCURATE QUANTUM COMPUTING

To be concrete, we examine the FTQC scheme of Ref. [11], built on idea of concatenating a QEC code put forth in earlier fault tolerance work. The analysis there forms the foundation of many subsequent FTQC proposals; our results are hence applicable to those based on concatenating codes. Such schemes have more well-established and complete theoretical analyses than some of the more recent developments like surface codes. They are hence a good starting point for our investigation here.

The scheme of [11], able to perform universal quantum computation, is built upon the 7-qubit code [12], using seven physical qubits to encode one (logical) qubit of information. We refer to the seven physical qubits used to encode the logical qubit as a “code block”, and gates on the logical qubit as “encoded gates”. At the lowest level of protection against errors, which we refer to as “level-1 concatenation”, each logical qubit is encoded using the 7-qubit code into one code block, and every computational gate is done as an encoded gate on the code blocks. Every encoded gate is immediately followed by a QEC box, comprising syndrome measurements to (attempt to) correct errors in the preceding gate. Faults can occur in any of the physical components—physical qubits and gates—including those in the QEC boxes, so the error correction may not always successfully remove the errors. Faulty elements in the QEC box may even add errors to the computer. A critical part of the construction of Ref. [11] is to ensure that the QEC boxes,

even when faulty, do not cause or spread errors on the physical qubits in an uncontrolled manner provided not too many faults occur, a realisation of the notion of fault tolerance.

At level-1 concatenation, the ability of the code to remove errors is limited. The 7-qubit code ideally removes errors in at most one of the seven physical qubits in the code block. To increase the QEC power, we raise the concatenation level of the circuit: Every physical qubit in the lower concatenation level is encoded into seven physical qubits; every physical gate is replaced by its 7-physical-qubit encoded version, followed by an QEC box. In this manner, level- k concatenation is promoted to level- $(k + 1)$ concatenation, for $k = 0, 1, 2, \dots$. The QEC ability of each level of concatenation increases in a hierarchical manner. For example, at level-2 concatenation, every logical qubit is stored in $7^2 = 49$ physical qubits organized into two layers of protection, with the topmost layer comprising seven blocks of seven physical qubits each. Each block of seven physical qubits is protected using the 7-qubit code; the 7 blocks of qubits are themselves protected by QEC in the second layer. This logic extends to higher levels of concatenation.

The concatenation endows the overall computational circuit with a recursive structure (see Fig. 2a), a crucial ingredient in the proof of the quantum accuracy threshold theorem. The increase in computational resource as the concatenation level grows is beneficial only if the increased noise due to the larger circuit is less than the increased ability to remove errors. This leads to the concept of a fault-tolerance threshold condition. The quantum accuracy threshold theorem gives a prescription for increasing the accuracy of quantum computation with no more than a polynomial increase in resources, provided the physical error probability is below a threshold level. Specifically, for the FTQC scheme of [11], the error probability per *logical* gate at level- k concatenation is upper-bounded by

$$p^{(k)} = \frac{1}{B}(B\eta)^{2^k}. \quad (1)$$

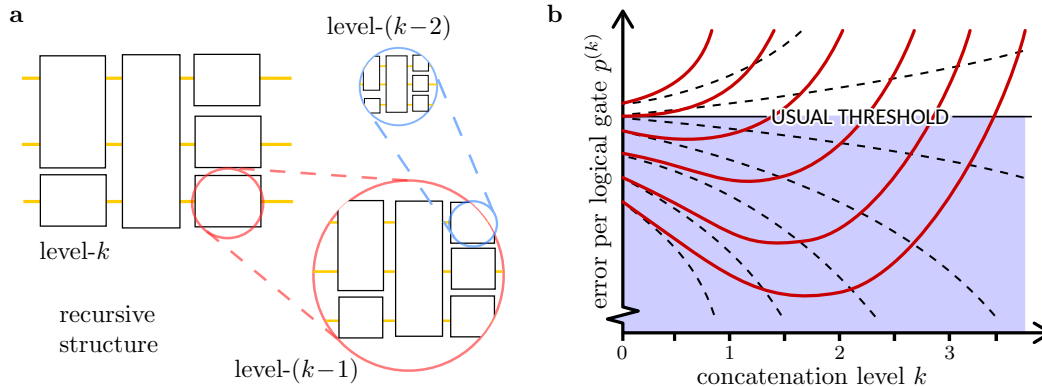


FIG. 2. **a**. The accuracy of a quantum computation can be increased by a FTQC scheme that makes use of concatenation and recursive simulation. Circuits are designed to be hierarchical, with high-level gate components built from lower-level components in a self-similar manner. **b**. A schematic diagram depicting the conventional situation (black dotted lines) where the physical error probability η is independent of the scale—the concatenation level k —of the computer, and our current consideration where η grows with k (red solid lines, each for a different value of $p^{(0)} \equiv \eta$). If η is k independent, standard FTQC analysis says that the error per logical gate $p^{(k)}$ can be brought as close to 0 as desired by increasing k , provided one starts below the threshold (solid horizontal line) at $k = 0$. If η depends on k , even if one starts below the threshold, $p^{(k)}$ eventually turns around for large enough k ; $p^{(k)}$ cannot reach 0, there is a maximum concatenation level, and further increase in k only increases the logical error.

Here, η is the *physical* error probability, and $p^{(0)} = \eta$. B is a numerical constant that captures the increase in complexity (number of physical components) of the circuit used to implement a single logical gate as one increases k for increased protection. Eq. (1) expresses quantitatively the idea of the accuracy threshold theorem: As long as

$$\eta < \frac{1}{B} \equiv \eta_{\text{thres}}, \quad (2)$$

$p^{(k)}$ decreases as k increases. Eq. (2) is the threshold condition, i.e., the physical error probability η in the quantum computer has to be below the threshold level η_{thres} for FTQC to work.

The double-exponential decrease in $p^{(k)}$ with k can be achieved [2–6, 10, 11] with only an exponential increase in resources, giving the no-more-than-polynomial increase in resource cost claimed in the accuracy threshold theorem. The number of physical gates in the circuit that implements the level- k logical gate is $G^{(k)} \equiv A^k$, where A is the number of physical gates in a level-1 encoded gate together with the QEC box. For the scheme of [11], one has $A = 575$ [13], and $B = \binom{A}{2} \simeq 10^5$. A more careful counting gives an improved value of $B \simeq 10^4$ [11].

The quantum accuracy threshold theorem assumes that the value of η , the physical error probability, remains constant even as the level of concatenation k increases. However, as mentioned, as k increases and the physical size of the computer grows, current experiments suggest that η also increases. Our goal here is thus to examine how the conclusions of the quantum accuracy threshold are modified if η itself grows with k . If η grows as k grows, intuitively, it is clear that, as k increases in an attempt to

reduce the logical error probability, the underlying noise per physical component increases to thwart that reduction. We will see that there is a maximum k beyond which further concatenation only serves to worsen the computational accuracy.

RESULTS

We examine the consequences of a k -dependent physical error probability $\eta^{(k)}$, illustrating it first with a toy model, before analysing the more realistic situation where a constraint on the total resource available for the computation leads to a shrinking amount of resource per physical gate as the computer scales up. The general effect of a k -dependent physical error probability can be summarized in the schematic Fig. 2b.

Toy model. We first illustrate this with a simple model in which $\eta^{(k)} = \eta^{(0)}(1 + ck)$, for $k = 0, 1, 2, \dots$, where $\eta^{(k)}$ is the physical error probability per gate in a computer large enough to perform level- k concatenation. Here, $c \geq 0$ and $\eta^{(0)} \geq 0$ are constants governed by the physical system in question. Although this is a toy model, one can think of it as the affine approximation of any $\eta^{(k)}$ function with weak k dependence, expanded about $\eta^{(k)} = \eta^{(0)}$. For this $\eta^{(k)}$, Eq. (1) gives

$$p^{(k)} = \frac{1}{B} \left[B\eta^{(0)}(1 + ck) \right]^{2^k} = p_0^{(k)}(1 + ck)^{2^k}. \quad (3)$$

Here, we define

$$p_0^{(k)} \equiv \frac{1}{B} \left(B\eta^{(0)} \right)^{2^k}, \quad (4)$$

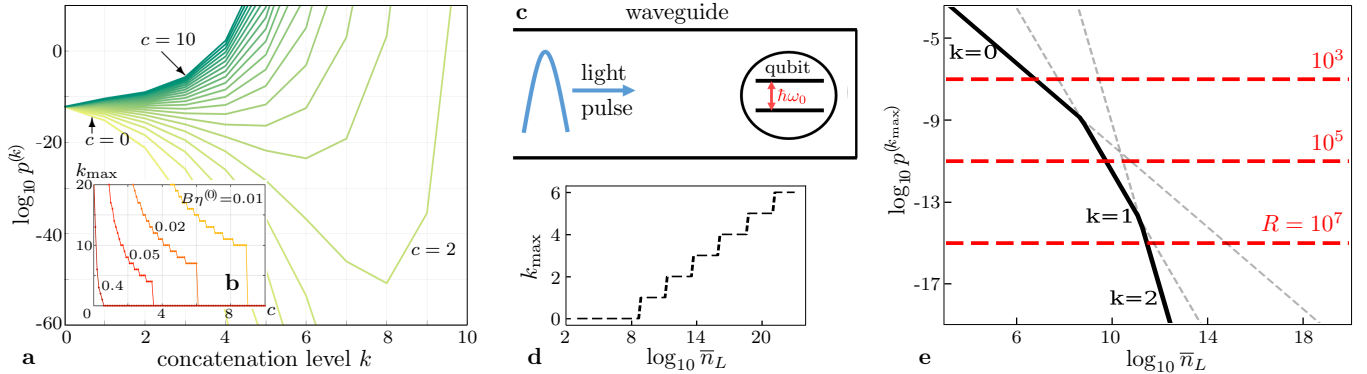


FIG. 3. **a.** An example of how $p^{(k)}$ varies as the concatenation level k increases, for the affine model with $c = 0$ (lightest color), $0.5, 1, \dots, 10$ (darkest color), $B = 10^4$ and $\eta_0 = 5 \times 10^{-6}$, for which $B\eta^{(0)} = 0.05$, far below the threshold for $c = 0$. All curves, apart from that for $c = 0$, turn around for large enough k . **b.** Maximum k value, k_{\max} , such that $p^{(k+1)} < p^{(k)}$, with $p^{(0)} \equiv \eta_0$, the unencoded error probability, for different values of $B\eta^{(0)} < 1$ and $c \in \{0, 0.1, 0.2, \dots, 10\}$. In every case, k_{\max} eventually falls to zero for large enough c , i.e., it is better to have no encoding. **c.** Qubit-in-waveguide schematic. **d.** k_{\max} as a function of number of photons per logical gate $\bar{n}_L = \bar{n}_{\text{tot}}/R^2$ (see text). **e.** Lowest possible error per logical gate $p^{(k_{\max})}$ as a function of $\bar{n}_L = \bar{n}_{\text{tot}}/R^2$, for the Shor's factoring algorithm. The horizontal red dashed lines correspond to the different target (p_{err}) values for different R values.

which would be the value of the error probability per logical gate if the error probability per physical gate were k independent. If $c = 0$, $p^{(k)}/p^{(k-1)} = p_0^{(k)}/p_0^{(k-1)} < 1$ as long as $\eta^{(0)} < 1/B$, as in Eq. (2); if $c > 0$, the multiplicative factor $(1 + ck)$ grows with k so, eventually, $p^{(k+1)} > p^{(k)}$ for k beyond some k_{\max} value. Corresponding to this maximum useful level of concatenation k_{\max} is the minimum attainable error probability $p_{\min} \equiv p^{(k_{\max})}$. Figure 3a shows an example of how $p^{(k)}$ varies as k increases, for different c values. As long as $c > 0$, $p^{(k)}$ decreases (if at all) before rising again, above some k_{\max} value.

Figure 3b shows the k_{\max} values for different c and $B\eta^{(0)}$ values (c.f. Fig. 2b). Clearly, k_{\max} decreases as c grows (stronger k dependence). Current experiments have $B\eta^{(0)} \gtrsim 1$; for example, the IBM Quantum Experience system has $\eta^{(0)} \gtrsim 10^{-3}$, giving $B\eta^{(0)} \gtrsim 10$ for $B = 10^4$. In near- to middle-term experiments, we expect $B\eta^{(0)}$ to not be far below 1, i.e., the error probability is just below the $c = 0$ threshold value [see Eq. (2)]. In this case, Fig. 3b suggests that one quickly loses the advantage of concatenating to higher levels even for small c values. In fact, for encoding to be helpful at all, i.e., for $k = 1$, we must have $p^{(1)} = B[\eta^{(0)}]^2(1+c)^2 < p^{(0)} = \eta^{(0)}$, which in turn requires

$$c < \frac{1}{\sqrt{B\eta^{(0)}}} - 1. \quad (5)$$

If $B\eta^{(0)} = 0.8$, say, this amounts to the requirement that $c \lesssim 0.1$, so that a very weak dependence on k is necessary for even one level of encoding to help at all in reducing the error probability.

General case. We can consider physical error proba-

bility that grows as *any* monotonic function of k : $\eta^{(k)} = \eta^{(0)}f(k)$, with $f(k) \geq 1$ a monotonically increasing function of k , and $f(0) = 1$. Then, the error probability per logical gate is $p^{(k)} = p_0^{(k)}f(k)^{2^k}$, where Eq. (4) gives $p_0^{(k)}$. Let $p^{(k)}$ attain its minimum at $k = k_{\max}$, with k now treated as a continuous parameter (or the nearest integer, in actual use). Straightforward algebra yields $k_{\max} < f^{-1}\left(\frac{1}{B\eta_0}\right)$ with $f^{-1}(\cdot)$ the inverse of $f(\cdot)$. If $f(k \rightarrow \infty)$ is finite, $p^{(k)}$ can be made arbitrarily small only if $\eta^{(0)} < [Bf(k \rightarrow \infty)]^{-1}$. However in many cases (such as the above toy model and the example in the following section), one has $f(k \rightarrow \infty) \rightarrow \infty$. Then the minimum $p^{(k)}$ will occur at finite k_{\max} , no matter how small $\eta^{(0)}$ is; one can never attain arbitrarily small logical error probability by concatenating further.

Total resource constraints. A realistic situation is one where η depends on the total number of physical components (qubits and gates) N in the computer. One expects the resource needed to maintain a given quality of physical gate operations to scale with N , so a constraint on the *total* available resource will result in a fall in the resource per physical component as the computer scales up. This gives a consequential drop in the quality of the gate, or, equivalently, a rise in the physical error probability η . A model that describes this situation is $\eta^{(k)} \propto N(k)^\beta$, for some positive constant exponent β , and a k -dependent N . For a concatenated FTQC scheme, we can set $N(k) = G^{(k)} = A^k$, so that the error probability per physical gate is

$$\eta^{(k)} = \eta^{(0)}A^{\beta k}, \quad (6)$$

with an exponential dependence on k . Then, the error

probability per logical gate is $p^{(k)} = p_0^{(k)} A^{\beta 2^k k}$, where Eq. (4) gives $p_0^{(k)}$. Going from $(k-1)$ to k levels of concatenation reduces the logical error probability when $p^{(k)}/p^{(k-1)} < 1$, satisfied for the model of Eq. (6) only when $k \leq k_{\max} < -\ln(B\eta^{(0)}A^\beta)/\ln(A^\beta)$, giving a minimum attainable logical error probability no smaller than $p^{(k_{\max})}$. Furthermore, we need $p^{(1)} < \eta^{(0)}$ for concatenation to be useful at all, i.e., $\eta^{(0)} < B^{-1}A^{-2\beta}$. This is often a much more stringent condition than $\eta^{(0)} < \eta_{\text{thres}}$ in Eq. (2); for example, if we take $A = 575$ as in Ref. [11] then for $\beta = 1$ one sees that $B^{-1}A^{-2\beta}$ is more than 10^5 times smaller than η_{thres} .

Example: Resonant qubit gates for factoring. As a concrete example of the above situation (with $\beta = 1$), we examine a resource constraint in a specific type of quantum gate implementation (see also a related early analysis in Ref. [14]). We consider qubits embedded in waveguides, i.e., continuums of electromagnetic modes prepared at zero temperature. Gates are activated by resonant propagating light pulses with a well-defined average energy, or, equivalently, an average photon number \bar{n}_g (see Fig. 3c). This describes the situation in superconducting circuits [15, 16] and integrated photonics [17]. It is also the paradigm of quantum networks and light-matter interfaces, with successful implementations in atomic qubits [18]. Here, we ask how an overall energetic constraint affects the efficacy of FTQC, and how to optimize the energy budget to realize a specific algorithm. For our illustrative goals, we treat only single-qubit gates subjected to noise from spontaneous emission. In doing so, we neglect the dephasing noise. While this is a fair approximation for atomic qubits, it is more demanding for solid-state qubits, but within eventual reach of superconducting circuits and spin qubits.

The qubit's dynamics follow the Lindblad equation, $\dot{\rho} = -\frac{i}{\hbar}[H(t), \rho] + \mathcal{D}(\rho)$, with the total Hamiltonian $H(t) = H_0 + H_D(t)$. Here, $H_0 \equiv -\frac{1}{2}\hbar\omega_0\sigma_z$ is the qubit's bare Hamiltonian, with $\sigma_z \equiv |0\rangle\langle 0| - |1\rangle\langle 1|$. The resonant drive induces the time-dependent coupling term $H_D(t) \equiv \frac{\hbar}{2}\Omega h(t)(|0\rangle\langle 1|e^{i\omega_0 t} + |1\rangle\langle 0|e^{-i\omega_0 t})$, with $h(t)$ a square function nonzero only for the duration of the gate: $h(t) = 1$ for $t \in [0, \tau]$ and 0 otherwise. Ω is the Rabi frequency, assumed to be much smaller than the qubit's natural frequency ω_0 , permitting the rotating wave approximation (RWA). The unitary evolution induced by this Hamiltonian is a rotation around the x-axis of the Bloch sphere by an angle $\theta = \Omega\tau$. This rotation is our single-qubit gate. In addition, the Lindblad dissipator $\mathcal{D}(\rho) \equiv \gamma(\sigma_-\rho\sigma_+ - \frac{1}{2}\{\rho, \sigma_+\sigma_-\})$ accounts for the spontaneous emission in the waveguide. Here $\sigma_- \equiv |0\rangle\langle 1|$ is the lowering operator, $\sigma_+ = \sigma_-^\dagger = |1\rangle\langle 0|$ the raising operator, and γ the spontaneous emission rate.

Note that Ω and γ are not independent, typical of waveguide Quantum Electrodynamics, where the driving and the relaxation take place through the same one-

dimensional electromagnetic channel. Spontaneous emission events while the driving Hamiltonian is turned on cause errors in the gate implementation. Their impact is reduced if the qubit is driven faster, i.e., if the Rabi frequency is larger. Conversely, the Rabi frequency is related to the mean number of photons inside the driving pulse through $\Omega = \frac{4\gamma}{\theta}\bar{n}_g$ (see Methods section). Pulses containing more photons thus induce better gates, with perfect gates for an infinite number of photons. The remnant noise, for a $\theta = \pi$ gate, has physical error probability (see Methods section) $\eta = \frac{\pi^2}{16}\frac{1}{\bar{n}_g}$. Note that the RWA upper bound on \bar{n}_g implies $\eta \geq \gamma/\omega_0$, the minimal noise for gate design within the RWA.

We now assume a constraint on the total number of photons \bar{n}_{tot} available to run the whole computation. As we show below, taking this constraint into account allows us to minimize the resource needed, for a target level of tolerable computational error. At level- k concatenation, the number of physical gates needed to implement a computation with L (logical) gates is $LG^{(k)} = LA^k$. Assuming a distinct pulse for each gate, the number of photons available per physical gate, given the total energetic constraint, is $\bar{n}_g = \bar{n}_{\text{tot}}(LA^k)^{-1}$. Thus, the physical error probability for the $\theta = \pi$ gate acquires an exponential k dependence,

$$\eta^{(k)} = \frac{\pi^2 LA^k}{16 \bar{n}_{\text{tot}}}. \quad (7)$$

Thus this is a concrete example corresponding to the $\beta = 1$ case in Eq. (6) above.

To better grasp the consequences of this k -dependent η , which we take as the generic behavior for all gates, we consider carrying out Shor's factoring algorithm [19]. Shor's factoring algorithm is touted as the reason the RSA public-key encryption system will be insecure when large-scale quantum computers become available. The current RSA key length is $R = 2048$ bits. The exponential speedup of Shor's algorithm over known classical methods comes from the fact that we can do the discrete Fourier transform on an R -bit string using $O(R^2)$ gates on a quantum computer (see, for example, Ref. [20]), compared to $O(R2^R)$ gates on a classical computer. The discrete Fourier transform gives a period-finding routine within the factoring algorithm, the only step that cannot be done efficiently classically. Thus, to run Shor's algorithm, one needs $L \sim R^2$ non-identity logical quantum gates for the discrete Fourier transform. The exact number of computational gates, including the identity gate operations which can be noisy, for the full Shor's algorithm depends on the chosen circuit design and architecture. For example, Refs. [21, 22] estimate $O(R^3)$ gate operations in total. Nonetheless, we will take the lower limit of $L \sim R^2$ in what follows. The concatenation values we find below are thus likely optimistic estimates.

A standard strategy is to demand that the computation runs correctly with probability $P_{\text{target}} > 1/2$; once

this is true, the computation can be repeated to exponentially increase the success probability towards 1. For $P_{\text{target}} = 2/3$, with L logical gates, each with error probability $p_{\text{err}} (\ll 1)$, we require $(1 - p_{\text{err}})^L > P_{\text{target}} = 2/3$, giving a target error probability per logical gate of $p_{\text{err}} \lesssim (3L)^{-1}$.

Fig. 3d presents the maximum concatenation level as an increasing function of the photon budget per logical gate $\bar{n}_L = \bar{n}_{\text{tot}}/R^2 (\sim \bar{n}_{\text{tot}}/L)$ (note: $\bar{n}_L = G^{(k)}\bar{n}_g = A^k\bar{n}_g$). It gives rise to Fig. 3e, the minimum attainable error per logical gate as a function of \bar{n}_L . Naturally, a larger R demands a larger photon budget to implement the algorithm. For the plotted choice of parameters, $R = 10^3$ requires no concatenation, and the required photon budget is $\bar{n}_L = 10^6$; for $R = 10^5$, we need $k = 1$ and $\bar{n}_L = 10^9$; for $R = 10^7$, we need $k = 2$ and $\bar{n}_L = 10^{11}$. Recall that, for the RWA to be applicable, as assumed in the design of the gates, we require $\omega_0 \gg \gamma\bar{n}_g$. For $R = 10^3$, this translates to the condition $\omega_0 \gg \gamma\bar{n}_g = \gamma\bar{n}_L/A^0 = 10^7\gamma$; for $R = 10^7$, we need $\omega_0 \gg 10^6\gamma$ for $A = 575$ (this A is from Ref. [11]). These conditions are attained for atomic qubits. They are within reach of future generations of superconducting qubits, where $\gamma \sim 10$ Hz for qubit frequency $\omega_0 \sim 10$ GHz. Today, the best coherence time for superconducting qubit is within the millisecond range: $\gamma \sim 1$ kHz [23, 24].

As an aside, our analysis also provides an estimate of the energy needed to run the gates involved in the Shor's algorithm, namely, $E_{\text{tot}} \sim \hbar\omega_0 L\bar{n}_L(R)$. For $R = 10^3$, with the above photon budget of 10^6 , this translates into $E_{\text{tot}} \sim 1$ pJ. Taking into account the parallelization of the computation (see Methods section), this corresponds to a typical power consumption of about 1 pW, while the $R = 10^7$ case requires only 10 nW of power. Note that these extremely low values do not take into account the low efficiency of the qubits' excitation, the specific requirements of particular physical architectures, or the cryogenic costs, the latter constituting the major part of the energetic bill. Nevertheless, the estimates point towards an energetic advantage of quantum nature, on top of the complexity advantage usually put forth to justify the interest in quantum computing technologies.

CONCLUSIONS

Given the current technical difficulties in experiments on quantum computing components, it appears likely that, in the near term, physical gate errors will rise as the number of qubits and the complexity of the implemented algorithm increase. This situation violates one of the basic assumptions of standard quantum fault tolerance analysis, that the physical error probability remains constant as the scale of the quantum computer grows. However, it is a natural consequence of the fact that as a physical device, a quantum computer is also impacted by the fact that physical resources are bounded.

Here, we explored the consequences of this violation

in increasing levels of practical relevance, from a toy example to illustrate the basic effects, to a realistic setting of qubits in waveguides. In every case, the standard tagline that fault-tolerant quantum computation allows us to go towards arbitrarily accurate quantum computers no longer holds. We find rapidly diminishing marginal returns as we try to scale up the computer size in an attempt to counter errors. The problem gets worse the closer the operating point is to the usual fault tolerance threshold given by Eq. (2).

Our analysis thus suggests two points of focus for experimenters working towards useful quantum computers: (1) to strive for weak scale dependence in the physical error probability; (2) to reduce the physical error probability significantly below the standard threshold level. Point (2) is anyway a requirement for standard fault tolerance to work well, for significant improvements per increase in scale (increase in k , for concatenated schemes), but gains further importance here with scale-dependent error probability. Point (1) may be difficult to attain, as long as there are significant practical limitations on the available resource for implementing the quantum computation. It motivates future study of efficient resource assignment and recycling [9], and reversible computing [25], to minimize the impact of resource constraints.

For concreteness, our work employs the fault-tolerance scheme based on the concatenated 7-qubit code. The qualitative, if not quantitative, conclusions, however, can be expected to hold even for other fault-tolerance schemes like that of surface codes, measurement-based schemes, etc. We illustrated our general analysis with the example of a constraint on the energetic budget to implement the gate operations. However, the same methodology can be applied to analyze the limits to quantum computation arising from constraints on other types of physical resources. Such analyses, beyond the scope of the present work, will be essential to assess the scalability of future large-scale quantum computers.

METHODS

We provide technical details pertinent to the qubit-in-waveguide example discussed in the Results section.

Resonant qubit gates. We consider a two-level system—the qubit—with bare Hamiltonian $H_0 = -\frac{1}{2}\hbar\omega_0\sigma_z$ embedded into a waveguide for light at resonant frequency ω_0 for implementing gate operations on the qubit. Assuming the system is at $0K$, and neglecting pure dephasing, the physics is described by the optical Bloch equations in which there is only spontaneous emission. The driving Hamiltonian is $H_D(t) \equiv \hbar\Omega h(t) \cos(\omega_0 t)\sigma_x$, writable in the form given in the main text, $H_D(t) \rightarrow \frac{1}{2}\hbar\Omega(t)(|0\rangle\langle 1|e^{i\omega_0 t} + |1\rangle\langle 0|e^{-i\omega_0 t})$ under the RWA. The overall qubit dynamics follows the Lindblad equation given in the main text: $\dot{\rho} = -\frac{i}{\hbar}[H(t), \rho] + \mathcal{D}(\rho)$,

with $H(t) \equiv H_0 + H_D(t)$ and $\mathcal{D}(\rho)$ the dissipator defined as $\mathcal{D}(\rho) = \gamma(\sigma_- \rho \sigma_+ - \frac{1}{2}\{\rho, \sigma_+ \sigma_- \})$.

The gate on the qubit is accomplished by an incoming coherent light pulse of power $P_{in} = \hbar\omega_0 \dot{N}_{in}$ where \dot{N}_{in} is the rate of incoming photons. The Rabi frequency induced by pulse is $\Omega = 2(\gamma \dot{N}_{in})^{1/2}$ [26]. It increases with γ , the time-constant for spontaneous emission, as both quantities measure the strength of the coupling between the qubit and the modes of the waveguide which provide both the decay and driving channels. As we are considering energetic constraints, i.e., a limit on the total number of photons to do gates, it is useful to express Ω in terms of the photon number \bar{n}_g available for that gate. For $H_D(t)$ describing a square pulse of duration τ with constant power, with \bar{n}_g available photons, $\dot{N}_{in} = \bar{n}_g/\tau$. In addition, to induce a rotation angle of θ , we require $\Omega\tau = \theta$, so that $\tau = \theta/\Omega$. We thus have $\Omega = 4\gamma\bar{n}_g/\theta$, and $\tau = \theta^2/(4\gamma\bar{n}_g)$ when expressed in terms of given \bar{n}_g and θ . Observe that, for a target θ , larger input energy, i.e., larger \bar{n}_g , enables faster gate operation.

The Lindblad equation, together with the expressions for Ω and τ in terms of θ and \bar{n}_g , describes the noisy implementation of a rotation of the qubit state by angle θ about the x axis in the Bloch ball, using given energy $\hbar\omega_0\bar{n}_g$. The noisy gate operation, $\tilde{\mathcal{G}}$, obtained by integrating the Lindblad equation over the gate duration τ , is a linear map that takes the input qubit state $\rho(t=0)$ to the (noisy) output state $\rho(t=\tau)$. It can be written in terms of the ideal gate \mathcal{G} as $\tilde{\mathcal{G}} = \mathcal{G} \circ \mathcal{E}$, with the noise map $\mathcal{E} \equiv \mathcal{G}^{-1} \circ \tilde{\mathcal{G}}$. \mathcal{E} is a completely positive (CP) and trace-preserving (TP) linear map, writable, using the Pauli operator basis $\{\mathbb{1}, \sigma_x, \sigma_y, \sigma_z\} = \{\sigma_\alpha\}_{\alpha=0}^3$ (with $\sigma_0 = \mathbb{1}, \sigma_1 = \sigma_x$, etc.), as

$$\mathcal{E}(\rho) = \sum_{\alpha, \beta=0}^3 \chi_{\alpha\beta} \sigma_\alpha \rho \sigma_\beta, \quad (8)$$

where $\chi_{\alpha\beta}$ are scalar coefficients.

The coefficients $\chi_{11} \equiv p_x, \chi_{22} \equiv p_y$, and $\chi_{33} \equiv p_z$ give the probabilities of X, Y , and Z errors, respectively, relevant for the 7-qubit code used in our discussion ($\chi_{\alpha\beta}$, with $\alpha \neq \beta$, do not affect the code performance; see, for example, Ref. [20]). Straightforward calculation gives $\frac{1}{2}\text{Tr}\{\sigma_\alpha \mathcal{E}(\sigma_\alpha)\} = \chi_{00} + \chi_{\alpha\alpha} - \sum_{\beta \neq 0, \alpha} \chi_{\beta\beta}$, for $\alpha = 0, 1, 2, 3$. We obtain p_x, p_y , and p_z by inverting these relations. For $\theta = \pi$, corresponding to the commonly used gate $\mathcal{G} = X(\cdot)X$, we find

$$p_x \simeq \frac{\pi^2}{16} \frac{1}{\bar{n}_g}, \quad p_y \simeq \frac{\pi^2}{32} \frac{1}{\bar{n}_g}, \quad \text{and} \quad p_z \simeq \frac{\pi^2}{32} \frac{1}{\bar{n}_g}, \quad (9)$$

accurate to linear order in $1/\bar{n}_g$. The largest of these, namely, p_x is what we set as η in the main text.

Energetic bill. Our analysis gives the energy required to carry out Shor's algorithm in a qubit-in-waveguide implementation, for a given problem size R : $E_{\text{tot}} =$

$\hbar\omega_0 L \bar{n}_L(R) \sim \hbar\omega_0 R^2 \bar{n}_L(R)$, where, as in the main text, $\bar{n}_L(R)$ is the number of photons required per logical gate operation for given R (and hence a given target logical error probability p_{err} ; see main text). $\bar{n}_L(R)$ can be read off Fig. 3e.

We can also estimate the average power cost, by assuming that all the logical gates in Shor's algorithm are run sequentially. Each logical gate is assumed to take M clock cycles per concatenation level; $M = 3$ for the scheme of Ref. [11]. The duration of a logical gate with k levels of concatenation is thus $\tau_L = M^k \tau_g$, with $\tau_g = \pi^2/(4\gamma\bar{n}_g)$ as the clock interval, taken to be the duration of the π -pulse gate analyzed above. The power P associated with the energy E_{tot} can hence be estimated as $E_{\text{tot}}/(L\tau_L)$. Some energetic numbers (orders of magnitude only) for the scheme of Ref. [11], with $\gamma = 10$ Hz and $\omega_0 = 10$ GHz, are given here:

	$R = 10^3$	$R = 10^5$	$R = 10^7$
Photon number \bar{n}_L	10^6	10^9	10^{11}
Concatenation level k	0	1	2
Energy E_{tot}	1 pJ	10 μ J	10 J
Power P	1 pW	1 nW	10 nW
Total time $L\tau_L$	100 ms	1000 s	10^9 s
Gate time τ_g	100 ns	100 ns	1 μ s

ACKNOWLEDGMENTS

This work is supported by a Merlion Project (grant no. 7.06.17), and by the Agence Nationale de la Recherche under the programme ‘‘Investissements d’avenir’’ (ANR-15-IDEX-02) and the Labex LANEF. HKN also acknowledges support by a Centre for Quantum Technologies (CQT) Fellowship. CQT is a Research Centre of Excellence funded by the Ministry of Education and the National Research Foundation of Singapore.

AUTHOR CONTRIBUTIONS

HKN formulated the question and worked out the toy model example; RSW worked out the general case with total resource constraints; AA and MFA worked out the energetic framework of quantum gates, and examined the details together with JHC. All authors contributed to the project discussion, and to the writing of the manuscript.

* huikhoon.ng@yale-nus.edu.sg

- [1] Arute, F. *et al.* Quantum supremacy using a programmable superconducting processor. *Nature* **574**, 505–510 (2019). URL <https://doi.org/10.1038/s41586-019-1666-5>.
- [2] Shor, P. W. Fault-tolerant quantum computation. In *Proceedings of 37th Conference on Foundations of Computer Science*, 56–65 (1996).

- [3] Kitaev, A. Y. Quantum computations: algorithms and error correction. *Russian Math. Surveys* **52**, 1191–1249 (1997).
- [4] Knill, E., Laflamme, R. & Zurek, W. H. Resilient quantum computation: error models and thresholds. *Proceedings of the Royal Society of London. Series A: Mathematical, Physical and Engineering Sciences* **454**, 365–384 (1998). URL <https://royalsocietypublishing.org/doi/abs/10.1098/rspa.1998.0166>.
- [5] Preskill, J. Reliable quantum computers. *Proceedings: Mathematical, Physical and Engineering Sciences* **454**, 385–410 (1998). URL <http://www.jstor.org/stable/53172>.
- [6] Aharonov, D. & Ben-Or, M. Fault-tolerant quantum computation with constant error rate. *SIAM Journal on Computing* **38**, 1207–1282 (2008). URL <https://doi.org/10.1137/S0097539799359385>. <https://doi.org/10.1137/S0097539799359385>.
- [7] Fowler, A. G., Mariantoni, M., Martinis, J. M. & Cleland, A. N. Surface codes: Towards practical large-scale quantum computation. *Phys. Rev. A* **86**, 032324 (2012). URL <https://link.aps.org/doi/10.1103/PhysRevA.86.032324>.
- [8] Monroe, C. & Kim, J. J. Scaling the ion trap quantum processor. *Science* **339**, 1164–1169 (2013). URL <https://science.sciencemag.org/content/339/6124/1164>.
- [9] Ikonen, J., Salmilehto, J. & Möttönen, M. Energy-efficient quantum computing. *npj Quantum Inf* **3**, 17 (2017).
- [10] Gottesman, D. *Stabilizer codes and quantum error correction*. Ph.D. thesis, California Institute of Technology (1997). ArXiv:quant-ph/9705052.
- [11] Aliferis, P., Gottesman, D. & Preskill, J. Quantum accuracy threshold for concatenated distance-3 codes. *Quantum Info. Comput.* **6**, 97165 (2006).
- [12] Steane, A. M. Error correcting codes in quantum theory. *Phys. Rev. Lett.* **77**, 793–797 (1996). URL <https://link.aps.org/doi/10.1103/PhysRevLett.77.793>.
- [13] Actually, $A = 575$ is the number of physical gate operations in an “exRec” for the CNOT gate, which includes the encoded gate operation together with its preceding, and trailing EC boxes. Furthermore, $G^{(k)}$ is more precisely given by $A(A')^{k-1}$ for $A' = 291$, the number of physical gate operations in a “Rec”, which includes the encoded gate together with its trailing EC box. These are details necessary to ensure the rigor of the quantum accuracy threshold theorem; the reader is referred to [11] for the full argument. They will, however, not change the qualitative features of our discussion, so we neglect them here.
- [14] Gea-Banacloche, J. Some implications of the quantum nature of laser fields for quantum computations. *Physical Review A* **65**, 022308 (2002).
- [15] Krantz, P. *et al.* A quantum engineer’s guide to superconducting qubits. *Applied Physics Reviews* **6**, 021318 (2019).
- [16] Peropadre, B. *et al.* Scattering of coherent states on a single artificial atom. *New Journal of Physics* **15**, 035009 (2013).
- [17] Lodahl, P., Mahmoodian, S. & Stobbe, S. Interfacing single photons and single quantum dots with photonic nanostructures. *Reviews of Modern Physics* **87**, 347 (2015).
- [18] Reiserer, A. & Rempe, G. Cavity-based quantum networks with single atoms and optical photons. *Rev. Mod. Phys.* **87**, 1379–1418 (2015). URL <https://link.aps.org/doi/10.1103/RevModPhys.87.1379>.
- [19] Shor, P. Algorithms for quantum computation: discrete logarithms and factoring. In *2013 IEEE 54th Annual Symposium on Foundations of Computer Science*, 124–134 (IEEE Computer Society, Los Alamitos, CA, USA, 1994). URL <https://doi.ieeecomputersociety.org/10.1109/SFCS.1994.365700>.
- [20] Nielsen, M. A. & Chuang, I. L. *Quantum Computation and Quantum Information: 10th Anniversary Edition* (Cambridge University Press, 2010).
- [21] Beauregard, S. Circuit for Shor’s algorithm using $2n + 3$ qubits. *Quantum Inf. Comput.* **3**, 175–185 (2003).
- [22] Häner, T., Roetteler, M. & Svore, K. M. Factoring using $2n+2$ qubits with toffoli based modular multiplication. *Quantum Inf. Comput.* **17**, 673–684 (2017). URL <http://www.rintonpress.com/xxqic/17/qic-17-78/0673-0684.pdf>.
- [23] Kjaergaard, M. *et al.* Superconducting qubits: Current state of play. *Annual Review of Condensed Matter Physics* **11** (2019).
- [24] Sears, A. P. *Extending Coherence in Superconducting Qubits: from microseconds to milliseconds* (Yale University, 2013).
- [25] Franck, M. P. Generalized reversible computing. In *Proceedings of the 9th Conf. on Reversible Computation* (2018).
- [26] Cottet, N. *et al.* Observing a quantum maxwell demon at work. *Proceedings of the National Academy of Sciences* **114**, 7561–7564 (2017).